PCCP

ARTICLE

Impact of Confinement in Multimolecular Inclusion Compounds of Melamine and Cyanuric Acid

Received 00th January 20xx,
Accepted 00th January 20xx

DOI: 10.1039/x0xx00000x

www.rsc.org/

Andre Nicolai Petelski,[a] Silvana Carina Pamies,[a] Agustín Gabriel Sejas,[a] Nélida María Peruchena,*[b,c] and Gladis Laura Sosa*[a,c]

Supramolecular cavities can be found in clathrates and self-assembling capsules. In these computational experiments, we studied the effect of folding planar hydrogen-bonded supramolecules of melamine (M) and cyanuric acid (CA) into stable cage-like quartets. Based on dispersion-corrected density functional theory calculations at the ωB97XD/6–311++G(d,p) level, we show the flexibility of M and CA molecules to form free confined spaces. Our bonding analysis indicates that only CA can form a cage which is more stable than their planar systems. We then studied the capacity of the complexes to host ionic and neutral monoatomic species like Na^+, Cl^- and Ar. The encapsulation energies range from –2 to –65 kcal mol^{-1}. A detailed energy decomposition analysis (EDA) support the fact that the triazine ring of CA is superior to the M one to capture chloride ions. In addition, the EDA and the topology of the electron density, by means of the Atoms in Molecules (AIM) theory and electrostatic potential maps, reveal the nature of the host-guest interactions in the confined space. The CA cluster appears to be the best multimolecular inclusion compound because it can host the three species by keeping its cage structure, and therefore could also act as a dual receptor of the ionic pair Na^+Cl^-. We think these findings could inspire the design of new heteromolecular inclusion compounds based on triazines and hydrogen bonds.

Introduction

Extramolecular, exomolecular, or multimolecular inclusion compounds are special cases within host-guest chemistry, in which more than one molecule creates the cavity for the guest complexation.[1] In this context, non-covalent interactions play a fundamental role. Firstly, they are responsible of keeping the cavity, and second, they hold the gust inside it. These systems have aroused a great volume of research[2,3] due to their promising applications; for instance, sequestration of small molecules, gases and ionic species.

Clathrates are the most well-known multimolecular inclusion compounds found in the crystal state, being hydroquinone clathrates the most representative ones. It has been shown that hydroquinone can form clathrates with several molecules and atomic species, like Xe,[4] hydrochloric acid,[5] carbon dioxide,[6] methanol and acetonitrile.[7] When clathrates are formed, a special arrangement of the multimolecular host is only stabilized due to the presence of the guest. This process is the result of a balance between attractive and repulsive forces. Takasuke Matsuo has indicated there is cooperative molecular recognition in the formation course,[1] and other authors have assumed there is no specific bond between the host and the guest molecules.[6] Nevertheless, M. Ilczyszyn *et al.*[8] have reported hydrogen bonds between the Xe atoms and the –OH groups that form the cavity within the famous Hydroquinone@Xe clathrates, which is a very specific interaction.

While metal-organic cages are widely known[2] and have found many applications,[9–11] hydrogen-bonded capsules are still in an early-stage advance. Rebek and coworkers have obtained, perhaps, the most prominent multimolecular host-guest complex: the *tennis ball*.[12,13] Among others, they have created several self-assembling capsules, with the ability of capturing small molecules like methane,[14] and even dimers.[15,16] Atwood[17,18] and Whitesides[19] have also mastered the supramolecular forces to create hydrogen-bonded capsules with enclosed spaces. In this context, triazine rings, like melamine and cyanuric acid, have shown to be suitable building blocks for creating supramolecular boxes in solution.[20]

Confinement using non-covalent interactions is also present in several host-guest systems, in which the host is a simple molecule. By far, calixarenes and cucurbituriles are the smallest molecules that can host atomic species and small molecules. Sashuk *et al.*[21] have obtained a square shaped molecule that can capture a single water molecule or a fluoride anion. Endohedral fullerenes are also a matter of study in this field. Very recently, it has been shown that the

[a] Grupo de Investigación en Química Teórica y Experimental (QuiTEx), Departamento de Ingeniería Química, Facultad Regional Resistencia, Universidad Tecnológica Nacional, French 414 (H3500CHJ), Resistencia, Chaco, Argentina.
[b] Laboratorio de Estructura Molecular y Propiedades, Facultad de Ciencias Exactas y Naturales y Agrimensura, Universidad Nacional del Nordeste, Avenida Libertad 5460, 3400 Corrientes, Argentina.
[c] Instituto de Química Básica y Aplicada del Nordeste Argentino, IQUIBA-NEA, UNNE-CONICET, Avenida Libertad 5460, 3400 Corrientes, Argentina.

Electronic Supplementary Information (ESI) available: [details of any supplementary information available should be included here]. See DOI: 10.1039/x0xx00000x

confinement of anions within C_{60} turns them into big anions.[22] Furthermore, the presence of cations was shown to drive the self-assembly of cavitands into multimolecular complexes.[23]

Chemical species have shown different properties when they are confined. For instance, in catalysis,[24] and hydrogen bonded systems.[25,26] Therefore, in this work we investigate the impact of folding planar supramolecules of M and CA into cage-shaped complexes. We focus on the stability of hydrogen bonds and the free confined spaces they hold. We then analyze the capacity of the triazine rings and the chemical spaces to capture monoatomic species like Na^+, Cl^- and Ar. Finally, through our computational experiments, we demonstrate herein that CA is a more robust building block for fabricating supramolecular inclusion compounds.

Computational Methods

All computations were performed with dispersion corrected density functional theory (DFT-D) implemented in the Gaussian 03 package,[27] by using the ωB97XD hybrid functional from Head Gordon *et al.*[28] with the 6-311++G(*d*,*p*) basis set. This method has proved to show a great performance in similar systems.[29–31] The minimum energy nature of the optimized structures was verified using the vibrational frequency analysis.

The bonding energies ΔE_{bond} (Equation 1) were obtained at the same level of theory using the approach of Fonseca Guerra *et al.*[32], which is calculated as the sum between the interaction energy of the complex ΔE_{int} and the deformation energy ΔE_{def}.

$$\Delta E_{bond} = \Delta E_{int} + \Delta E_{def} \quad (1)$$

In this equation, the interaction energy ΔE_{int} is the difference between the energy of the complex and the sum of energies of the monomers with the structures that take place in the complex. The deformation energy ΔE_{def} is the energy needed to deform the structure of monomers from their isolated state to that one they acquire in the complex. The ΔE_{int} of the inclusion compounds was further decomposed into encapsulation energy ΔE_{enc} and hydrogen bonding energy ΔE_{HB} according to equations 2 – 4.

$$\Delta E_{int} = E_{cage@A} - \sum E_m - E_A \quad (2)$$
$$\Delta E_{int} = \left(E_{cage@A} - E_{cage} - E_A\right) + \left(E_{cage} - \sum E_m\right) \quad (3)$$
$$\Delta E_{int} = \Delta E_{enc} + \Delta E_{HB} \quad (4)$$

Here, $E_{cage@A}$ is the energy of the multimolecular inclusion compound (with A = Na^+, Cl^-, Ar), E_m is the energy of the monomers (either M or CA) and E_A is the energy of the host; then E_{cage} is the energy of the system without the guest, with the geometry of cage@A. All the interaction energies were corrected for the basis set superposition error (BSSE) within the counterpoise method of Boys and Bernardi.[33]

The non-covalent interactions were analyzed within the framework of the Atoms in Molecules theory. Total electron densities were calculated at the same level of theory. The local properties at the bond critical points were computed using the AIMALL program.[34] Molecular electrostatic potential surfaces were generated by mapping the electrostatic potential *V*(r) on the electronic density surfaces. We considered an isosurface of ρ(r) = 0.001 au, which was suggested by Bader *et al.*[35] and represents the effective molecular volume.

The interactions between the host and the isolated guests were also analyzed with the localized molecular orbital energy decomposition[36] (LMOEDA) method at the BLYP-D3/6-311++G(d,p) level of theory, using the GAMESS[37] quantum chemistry package. This method partitions the interaction energy into four components, according to equation 5:

$$\Delta E_{int} = \Delta E_{ele} + \Delta E_{ex-rep} + \Delta E_{pol} + \Delta E_{disp} \quad (5)$$

where the term ΔE_{ele} describes the classical electrostatic interaction (Coulomb) of the occupied orbitals of one monomer with those of another monomer; $\Delta E_{ex\text{-}rep}$ is the attractive exchange component resulting from the Pauli exclusion principle and the interelectronic repulsion; ΔE_{pol} accounts for polarization and charge transfer components; and ΔE_{disp} corresponds to the dispersion term.

Results and Discussion

Geometries and relative stabilities

We started from the planar complexes. Then, the cage-like clusters were built by folding the planar ones in order to form cyclic quartets, and keeping the original hydrogen bonds (H-bonds). The structures of the systems are shown in Figure 1, and the corresponding energies are displayed in Table 1. All the cages assume a C_2 symmetry. When folding the planar systems into cyclic quartets, two extra H-bonds are formed (or three in the case of M_2CA_2). Therefore, one may expect a stronger bonding energy in the later. However, there is an energy penalty related to the acceptor directionality of the H-bond.[38] Although the differences in interaction energies are around 5 kcal mol^{-1}, ΔE_{bond} values show there is no extra stabilization. The only exemption is the second cage of CA (CA_4-2), which is 4.8 kcal mol^{-1} more stable than its planar counterpart. The formation of the cages also requires a deformation energy, which is almost cero for CA_4-2 and relatively high for M_4 and M_2CA_2.

Finally, the Gibbs free energies of bonding shows that the planar systems are by far the most stable ones. In the case of CA_4-2, the planar and cage systems differ in just 0.8 kcal mol^{-1}. Therefore, these results point out again that this cage-like cluster is the most viable one.

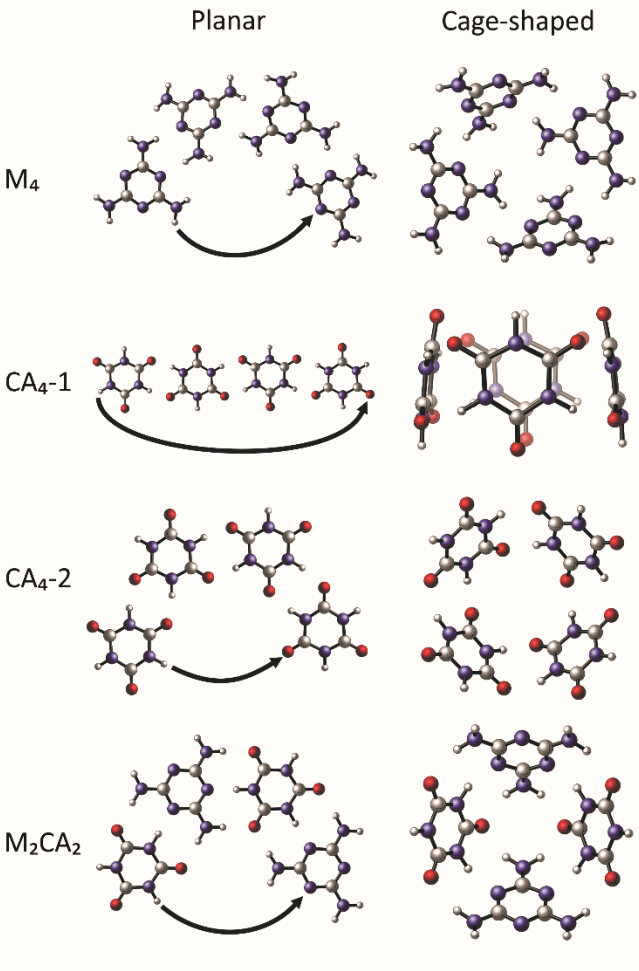

Fig. 1 Optimized geometries at ωB97XD/6–311++G(d,p) level of theory. Black arrows indicate the folding of the planar systems.

Table 1 Bonding and interaction energies (kcal mol^{-1}) calculated at ωB97XD/6–311++G(d,p) level of theory.

System	Type	ΔG_{bond}	ΔE_{bond}	ΔE_{def}	ΔE_{int}
M_4	Planar	0,7	–39.6	0.8	–40.4
	Cage	6,9	–40.1	4.6	–44.7
CA_4-1	Planar	–6,9	–40.9	1.2	–42.1
	Cage	0,2	–40,6	–0.5	–40.1
CA_4-2	Planar	–6,4	–41.6	1.0	–42.6
	Cage	–5,6	–46,4	0.7	–47.1
M_2CA_2	Planar	–21,4	–60.0	4.5	–64.5
	Cage	–13,3	–60.8	7.4	–68.2

Topology of the cavities

All the cage-shaped quartets form regular cavities with a cup-like shape akin to that of calixarenes. From their molecular electrostatic potentials maps shown in Figure 2 (a and b), it can be seen that the inside is more positive than the outside surface. According to this, the CA_4-1 cage creates the most positive cavity, followed by CA_4-2, the mix complex of M_2CA_2 and M_4. In order to gain more information of the cavities we then obtained sections of the electron densities ρ(r), which are also plotted in Figure 2 (c). As shown in Figure 2, M_4, CA_4-2 and M_2CA_2 display a cup-like shape, which are quite similar to some calixarenes.[39,40] Furthermore, CA_4-1 complex shows a cage-like cluster with a tubular cavity, alike that observed in the pillar[4]pyridinium molecular box.[21] This suggests that linear molecules like H_2 could fit inside the cavity.

Table 2 reports some meaningful topological parameters of H-Bonds. That is, the electron density ρ at the BCPs, that reflects the strength of a bond. The total energy density $H = G + V$, where G and V are the kinetic and potential energy densities respectively. The ellipticity ε, that measures the extent of the electron density within a plane containing the line path. In addition, it is a direct measure of the stability of a given bond, because it takes infinite large values preceding the coalescence of a ring critical point and a BCP.[41] The delocalization [δ(A,B)] index, which is a measure of the number of electrons that are shared or exchanged between A and B. Finally, the repulsive part of the local potential energy density V_{rep} that accounts for electron-electron and nuclear-nuclear repulsion.

PCCP

ARTICLE

Table 2 Values of local topological properties (a.u.) at the bond critical points.[a]

Complex	Type	Atoms	ρ	H	ε	δ(H,N/O)	V_{rep}
M_4	Planar	H···N	0.029	0.001	0.073	0.096	0.888
	Cage	H···N	0.024	0.001	0.093	0.081	0.782
CA_4-1	Planar	H···O	0.031	0.001	0.033	0.087	0.914
	Cage	H···O	0.023	0.002	0.026	0.068	0.777
CA_4-2	Planar	H···O	0.032	0.001	0.032	0.089	0.985
	Cage	$H\cdots O_{up}$[b]	0.022	0.003	0.041	0.064	0.695
		$H\cdots O_{down}$[c]	0.032	0.001	0.032	0.086	1.088
M_2CA_2	Planar	H···O	0.025	0.002	0.051	0.076	0.759
		H···N	0.045	-0.007	0.065	0.138	1.507
	Cage	$H\cdots O_{up}$	0.018	0.002	0.078	0.056	0.533
		$H\cdots N_{middle}$[d]	0.033	-0.001	0.096	0.108	1.188
		$H\cdots O_{down}$	0.021	0.002	0.092	0.062	0.744

[a] Due to symmetry reasons, average values are shown. [b] The sub index *Up* corresponds to the average values of the largest opening. [c] The sub index *Down* corresponds to the average values of the smallest opening. [d] *Middle* corresponds to hydrogen bonds positioned at the middle of the cup-like structure.

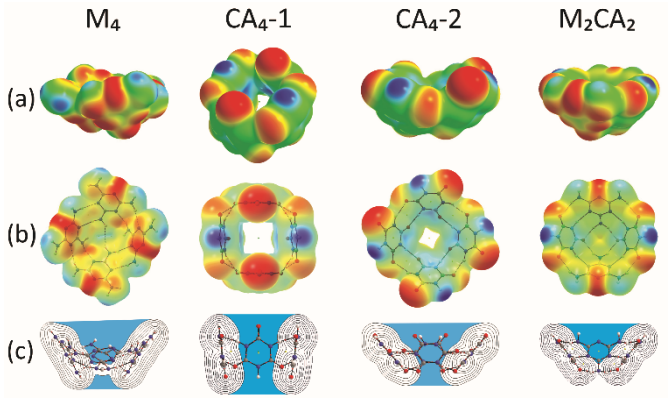

Fig. 2 (a) Side views of molecular electrostatic potentials (MEPs) maps on the 0.001 a.u. electron density isosurfaces. (b) Top views of MEPs. The values of the MEP vary between –31 kcal mol^{-1} (red) and 56 kcal mol^{-1} (blue). (c) Contour plots of cage-shaped complexes superimposed to molecular graphs. The free space is colored at light blue.

When going from the planar systems to the cage-like structures, H-Bonds undergo an important bending. This deformation has an impact on the acceptor directionality,[42] and it is clearly reflected in their topological values (see Table 2). According to ρ, the strength of the bond decreases with the bending along with a decrease in δ(H,N/O). The ellipticity also increases, except in AC_4-1. The fact that the cup-like structure of AC_4-2 is more stable than the planar form can be undoubtedly understood by looking the topological parameters. The AC_4-2 cup-shaped complex forms 8 H-bonds, four within the largest opening ($H\cdots O_{up}$) and four below it ($H\cdots O_{down}$), having different topological properties. As can be seen from Table 2, the bending does not significantly affect the H-bond properties of the smallest opening, if we compare them with the planar system. Therefore, the two extra H-bonds that are formed in the cage complex are enough to compensate the decrease in interaction energy do to the directionality.

Encapsulation effect

As was shown above, all the cage-shaped complexes form regular cavities that could host atomic species, or even linear molecules. Therefore, we put them to test with ionic and neutral species like sodium, chloride and argon. All the systems were fully optimized, and those who kept their original shape were reported. Table 3 shows the bonding analysis of the multimolecular inclusion complexes. Gibbs free energies and bonding energies are more stabilizing with the presence of the hosts, except for M_4@Ar and and AC_4-1@Ar. Among all the complexes, just CA_4-2 can host a sodium cation and keep its original shape, being the encapsulation energy the greatest one.

Concerning chloride, the greatest ΔE_{enc} is shown for CA_4-1, followed by CA_4-2, M_2CA_2 and M_4. This trend suggests that the triazine skeleton of CA is better than the melamine one to capture anions, which could be used for synthesizing new heterocalixarenes. In this context, Frontera *et al.* have already shown experimental evidence of chloride-π interactions in CA crystals.[43] The deformation energies are also more favorable for CA complexes. For the sake of comparison, we then computed the corrected interaction energy (ωB97XD/6-311++G(d,p)//BP86/TZ2P) for an heterocalixarene-chloride complex recently reported by Caramori *et al.*[44] (see compound **1**·Cl$^-$). The complex gives an encapsulation energy of –31.8 kcal mol^{-1} (BP86/TZ2P energy[44] is –37.6 kcal mol^{-1}), which is

very close to those informed in Table 3, and even smaller. Finally, since the second cage of CA can host both ions Na^+ and Cl^-, one may think that this system could host both ions at the same time. Indeed, we optimized the CA_4-2 system with the NaCl ionic pair and the complex keeps its original shape (see Figure S1). The ΔE_{enc} is −55.7 kcal mol^{-1} (value not informed in the Table), and the ΔE_{def} is even lower than for the isolated ions (1.6 kcal mol^{-1}).

When an argon atom is placed within the cavity, the most favorable values are, again, those for CA complexes, as shown in Table 3. That is, high encapsulation energies and low deformation energies.

Table 3 Bonding analysis (kcal mol^{-1}) of multimolecular inclusion compounds obtained at ωB97XD/6–311++G(d,p) level of theory.

Complex	Guest	ΔG_{bond}	ΔE_{bond}	ΔE_{def}	ΔE_{int}	ΔE_{HB}	ΔE_{enc}
M_4	Cl^-	−8.3	−66.6	12.1	−78.7	−44.1	−34.5
	Ar	10.3	−44.1	4.3	−48.4	−45.0	−3.4
CA_4-1	Cl^-	−40.4	−92.0	2.3	−94.3	−40.3	−54.0
	Ar	2.0	−45.0	−1.1	−43.9	−40.1	−3.8
CA_4-2	Na^+	−51.2	−102.6	6.6	−109.2	−44.8	−64.3
	Cl^-	−37.0	−88.3	3.1	−91.3	−45.2	−46.2
	Ar	−2.6	−49.7	0.2	−49.9	−47.1	−2.8
M_2CA_2	Cl^-	−39.0	−97.6	10.9	−108.4	−66.8	−41.6
	Ar	−9.6	−64.9	7.0	−71.9	−68.4	−3.5

Confined interactions

LMOEDA Before evaluating the forces that take part in the encapsulation, we must know the nature of the interactions between the atomic species and the isolated triazines. Therefore, we computed a potential energy scan by varying the distance (***r***) between Cl^-/Ar and the triazine ring center. The systems were optimized with C_3 symmetry, and the ***r*** distance was varied from 2.7 Å to 3.4 Å with a 0.05 Å step (15 optimizations). We then decomposed the interaction energy in every step and the profile for chloride is plotted in Figure 3 (see energy profile for argon in Figure S2).

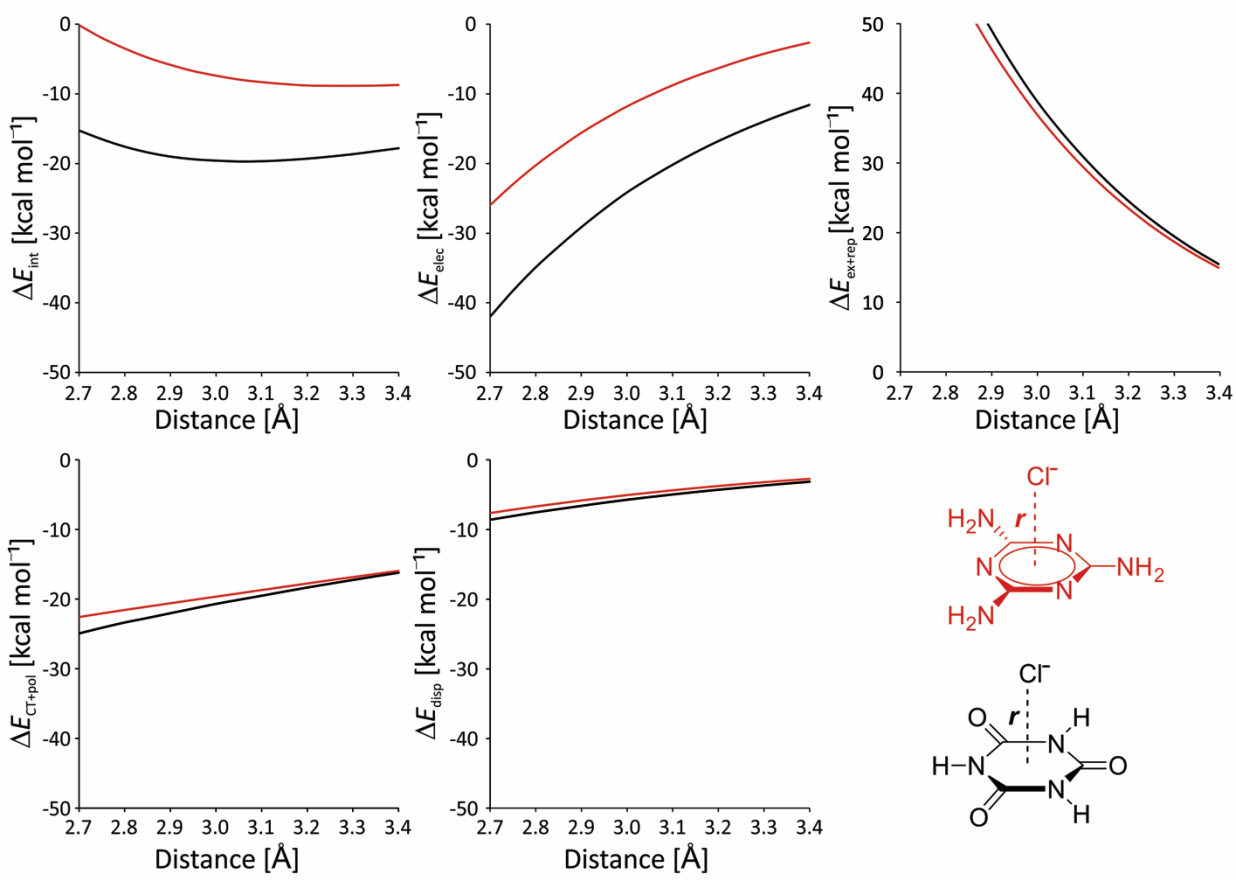

Fig. 3 Variation of LMOEDA energy components as a function of ***r***. Chemical structures of the scanned systems are shown, where ***r*** is the scanned distance.

At first glance, chloride interacts more strongly with CA than M along all the scanned distance. At the equilibrium geometry, the interaction energy with M is −8.7 kcal mol^{-1} and −19.7 kcal mol^{-1} with CA. The profile of the energy

components indicates that the electrostatic part is the dominant factor of the interaction energy. In addition, the interaction between Cl^- and CA has larger charge transfer and dispersion components. These results are in agreement with the trends of encapsulation energies, reaffirming therefore, the fact that the CA skeleton is a better candidate for synthesizing molecular hosts based on triazines.

Concerning the interactions with argon, the differences in interaction energies are negligible (the energy profiles are shown in supporting information).

When these interactions are confined in the cavity, its nature changes drastically. Table 4 collects the LMOEDA analysis of all complexes. In general, the attractive nature of the encapsulation is mostly explained by the charge transfer component. For instance, the interaction of chloride with CA goes from 46% electrostatic in the non-confined state to 5.6% in the CA_4-1 complex. The other complexes show repulsive electrostatic interactions, and the trend follows observation of Figure 2 (CA_4-2 < M_4 < M_2AC_2). The fact that the M_4@Cl^- cage show a larger charge transfer contribution is due to the presence of N–H···Cl^- hydrogen bonds that hold the anion. Moreover, the Pauli repulsion is again larger for the systems with M, and the dispersion component is almost the same for all the systems.

All of these interaction energy components lead us to think that the CA molecule will be the best choice. Not only because an improved interaction energy with the ions but also because this fact will most likely guide the process to the target system. In the beginning of the assembly, the process will be under the control of the electrostatic energy. When the cage is formed, the ion will be held by stronger orbital interactions than in the free state. Of course, one has to think that all the cages should be equipped with functional groups to improve the stabilization. In order to pre-induce complexation,[19] another approach could be the joint attachment between two or more monomers.

Table 4 Energy decomposition analysis (in kcal mol^{-1}) of equilibrium geometries obtained at BLYP-D3/6-311++G(d,p)

Complex	Guest	ΔE_{ele}	ΔE_{ex-rep}	ΔE_{pol}	ΔE_{disp}	ΔE_{int}
M	Cl^-	-2.90	13.08	-16.12	-2.81	-8.74
	Ar	5.69	2.90	-8.62	-1.35	-1.38
CA	Cl^-	-21.52	26.98	-19.93	-5.23	-19.71
	Ar	6.11	2.94	-9.16	-1.39	-1.51
M_4	Cl^-	5.58	63.46	-93.33	-11.45	-35.45
	Ar	48.46	8.94	-58.03	-3.93	-4.55
AC_4-1	Cl^-	-4.92	34.76	-75.35	-7.71	-53.22
	Ar	44.79	10.1	-55.82	-4.63	-5.56
AC_4-2	Cl^-	0.03	31.73	-70.88	-6.99	-46.11
	Ar	42.78	6.49	-50.31	-3.02	-4.05
M_2CA_2	Cl^-	7.78	45.53	-86.24	-8.61	-41.46
	Ar	51.65	9.40	-61.78	-4.18	-4.91

QTAIM When either chloride or argon is approached to the triazine ring, interactions with the π system are expected.[44,45] In the framework of the QTAIM, a bond path is a line of maximum electron density that links a pair of nuclei,[46,47] within an equilibrium geometry. When looking the $L(r)$ function ($-\nabla^2\rho$) of M and CA (Figure 4), a nonbonding charge concentration (NCC) over N atoms and a hole over C can be observed. Note that the NCCs correspond to the Lewis model of lone pairs. In the triazine ring of CA, the lone pairs of N appear delocalized. Therefore, BCPs between either Cl^- or Ar and N atoms would be likely to be present. Figure 5 shows the molecular graphs of complexes M···Cl^-/Ar and CA···Cl^-/Ar, in which BCPs between Cl^-/Ar and N atoms are observed; and Table 5 reports the average properties of those BCPs. The reported values are characteristic of weak closed-shell interactions: low values of ρ, positive laplacian $\nabla^2\rho$ and $H \approx 0$. Since ρ and δ(A.B) are good indicators of the bond strength, their values are in line with the interaction energies. In addition, V_{rep} is more repulsive for CA···Cl^-, as was shown in the previous section. Observations regarding Argon indicate there are no significant differences between M and CA.

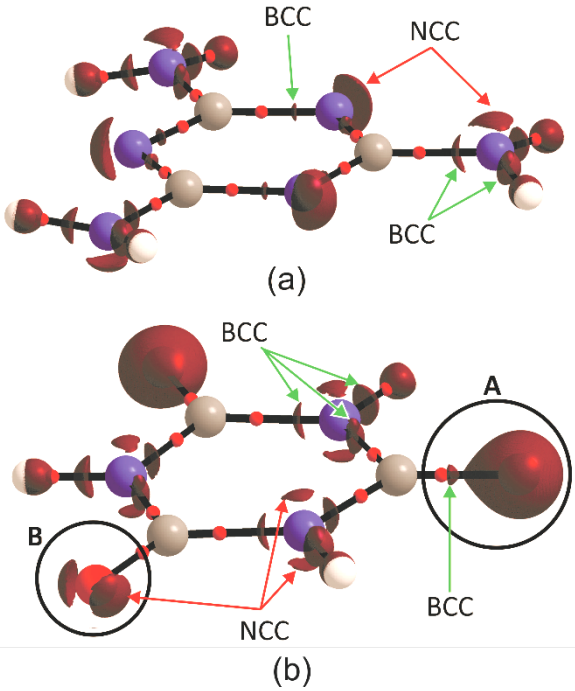

Fig. 4 Three-dimensional isosurfaces of $L(r)$ = 1.5 a.u. for (a) melamine and (b) cyanuric acid. Circles **A** and **B** correspond to $L(r)$ = 1.03 and 3.0 respectively. Bonding (BCC) and nonbonding charge concentrations (NCC) are indicated with arrows.

Table 5 Local topological properties at N···Cl^-/Ar bond critical points[a] (a.u.)

Complex	Atoms	ρ	$\nabla^2\rho$	H	ε	δ(A.B)	V_{rep}
CA···Cl^-	N···Cl^-	0.009	0.029	0.001	2.343	0.064	0.189
CA···Ar	N···Ar	0.003	0.011	0.001	0.370	0.017	0.055
M···Cl^-	N···Cl^-	0.006	0.016	0.001	3.416	0.040	0.104
M···Ar	N···Ar	0.003	0.011	0.001	1.216	0.015	0.052

[a] Average values of bond critical points.

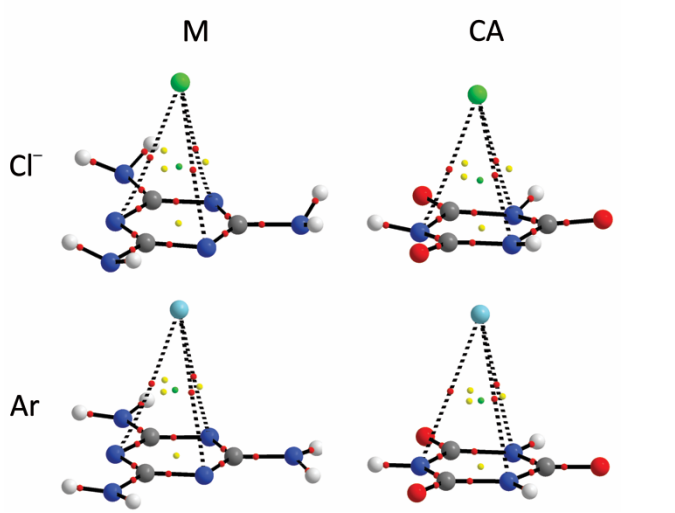

Fig. 5 Molecular graphs of M···Cl^-/Ar and CA···Cl^-/Ar complexes. Small *red* dots are BCP, *yellow* dots are ring critical points and *green* dots are cage critical points.

It is worth to note that some meaningful QTAIM parameters (ρ, ESP, V_{rep} and charge transfer) are straight related to LMOEDA terms (ΔE_{int}, ΔE_{ele}, ΔE_{ex-rep}, ΔE_{pol} and ΔE_{disp}), as shown in Figures S3-S6 in supporting information. These relationships were obtained by computing the local topological properties over the scanned systems, which were discussed above. For instance, among other relationships between EDA components and AIM parameters,[48,49] it has been shown that there is a linear relationship between ρ and the interaction energy.[50,51] However, we found herein a quadratic relationship between these two parameters. In addition, the sum of the ESPs at the BCPs vs. ΔE_{ele}, and the charge transfer obtained by QTAIM vs. ΔE_{pol} were found to be linearly correlated for both CA···Cl^- and M···Cl^- systems. In the case of Argon, the charge transfer values obtained with the QTAIM fails to describe its behavior. Previous studies on Voronoi Deformation Densities have shown that Bader's charges fail to describe some systems.[52] Nevertheless, according to those relationships, the topological properties can be used to monitor either the strength, electrostatic and repulsive features of the interactions.

Now that we have identified the nature of the interactions between the atomic species and M and CA isolated rings, we analyse the situations within the cavities. Figure 6 shows the molecular graphs of the multimolecular inclusion compounds, and topological properties of the inclusion interactions are reported in Table S1 (supporting information). The presence of BCPs between the multimolecular hosts and the guests clearly show the encapsulation effect. They show typical values of weak closed-shell interactions. The values of ρ (BCP) are within the range of 0.004–0.023 a.u. for the systems with chloride and 0.003–0.004 a.u. for the systems with argon. The H-Bonds that keep the cavity are also intact, and their topological properties do not change significantly (see Table S2). When the M···Cl^-/Ar and CA···Cl^-/Ar interactions are confined, their topological properties display a different behavior. These changes are consistent with those observed in the LMOEDA analysis. For instance, the interactions with chloride are weaker than those of chloride with the isolated rings. Nevertheless, the presence of multiple bond paths increases the interaction energy. Interestingly, in some cases, the BCPs appear between C atoms and the guests, instead of N (e.g., CA_4-2). In the case of M_4@Cl^-, the anion is also held by N–H···Cl^- H-Bonds. It is also interesting to point out that, in most of the cases, the host-guest N···Cl^- interactions show significant lower values of ellipticity (ε) when they are compared with the non-confined values. This might indicate the interactions are more stable within the cage. Furthermore, when comparing CA_4-1@Cl^- and CA_4-2@Cl^- the sum of ρ and δ(A.B) are in line with the encapsulation energies ΔE_{enc}. The repulsion ($\sum V_{rep}$) is also greater for the CA_4-1@Cl^- complex, ~~also~~ in agreement with values of Table 4. Even though we cannot address strong conclusion regarding the character of the interactions, what is evident herein are the differences between the confined and non-confined states. The multimolecular hosts produce a chemical space with an environment that is totally different from the separate triazine rings.

On the other hand, the CA_4-2 cage is the only system that can capture Na^+ without losing the original cup structure. The cation is tetracoordinated, and the BCPs show values that are characteristic of closed-shell interactions as well: low values of ρ, and positive values of $\nabla^2\rho$ and H. According to Bader, this type of interaction cannot be classified as a metal coordination.[53] Furthermore, the same system (CA_4-2@Na^+) can simultaneously hold chloride, that is, CA_4-2@NaCl. Its molecular graph (Figure 7), show a different topology for chloride. In this complex, the anion is pushed down the cavity because of the presence of the cation. Consequently, the anion interacts less with the π cloud of CA. This topology can be clearly understood by looking the laplacian of the electron density (Figure S7). Note that the encapsulation energies for the separate ions Na^+ and Cl^- are –64.3 and –46.2 kcal mol^{-1},

respectively (Table 3). However, the encapsulation energy of the ionic pair is just −55.7 kcal mol^{-1}. This suggest that the whole encapsulation energy of NaCl might just come from the coordination of Na^+ counter ion.

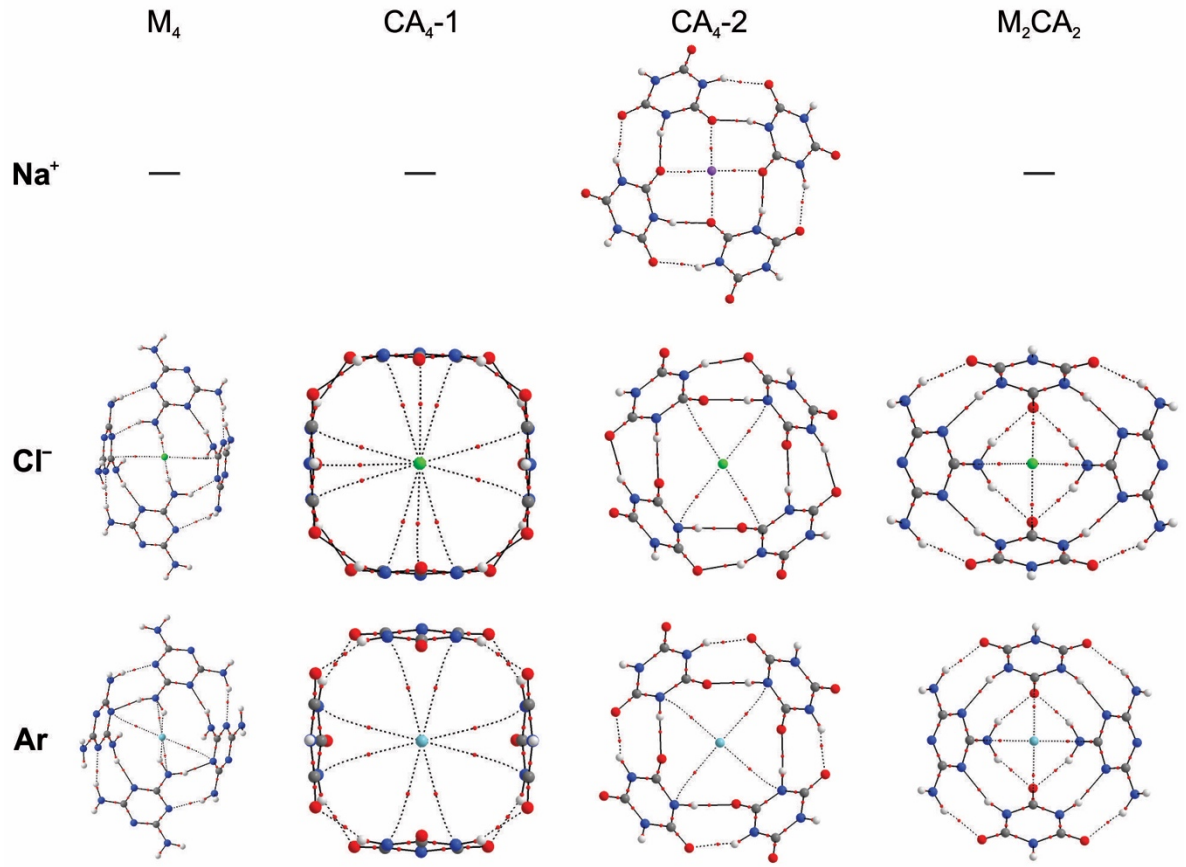

Fig. 6 Molecular graphs of multimolecular inclusion compounds.

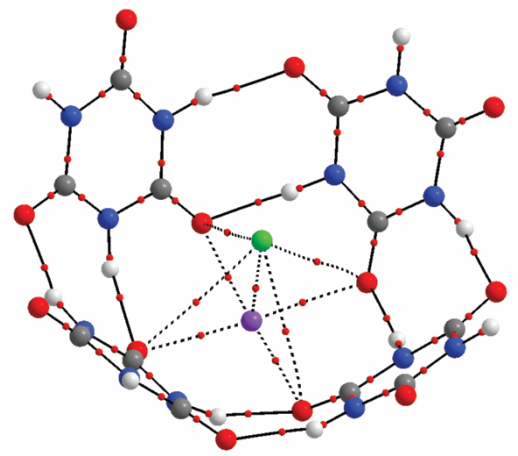

Fig. 7 Molecular graph of CA cage-shaped cluster acting as a dual receptor of sodium cation and chloride.

Conclusions

In this work, we have conducted a DFT-D analysis over a set of multimolecular inclusion compounds based on M and CA. Our study has shown that these molecules are able to form confined cavities alike calixarenes with the ability to host small atomic species. Whilst the cavity is created by hydrogen bonds, in most of the cases the guest species are encapsulated due to the interactions with the π systems of melamine and cyanuric acid. Nevertheless, melamine can retain the anion with its amino groups (N–H···Cl$^-$), while cyanuric acid can coordinate cations with its keto groups (C=O···Na$^+$).

Our bonding analysis suggests that only one cage-shaped supramolecule of CA is more stable than its open structure by ~5 kcal mol^{-1}. In the other cases, the extra hydrogen bonds, which are created in the cyclic complexes, are not enough to compensate the weakening of the interactions due to the bending. The triazine skeleton of CA was also shown to be more robust to capture an ionic guest. In addition, our computations suggest that CA could act as a dual receptor of ionic pairs. Therefore, with proper covalent modifications, CA seems to be the most versatile building block for synthesizing supramolecular inclusion compounds via hydrogen bonds. Nevertheless, the other cage-shaped structures could serve as model sets for constructing new heteromolecular hosts.

Conflicts of interest

There are no conflicts to declare.

Acknowledgements

The authors gratefully acknowledges the financial support from the Secretaría de Ciencia y Tecnología, Universidad Tecnológica Nacional, Facultad Regional Resistencia. A.N.P. thanks the National Scientific and Technical Research Council (CONICET), Argentina, for a doctoral fellowship. N.M.P. is a CONICET career researcher.

Notes and references

‡ Footnotes relating to the main text should appear here. These might include comments relevant to but not central to the matter under discussion, limited experimental and spectral data, and crystallographic data.
§
§§
etc.

1 J. L. Atwood and J. W. Steed, Eds., *Encyclopedia of Spramolecular Chemistry. Vol 1*, CRC Press, Boca Raton, 2004.
2 M. Yoshizawa, J. K. Klosterman and M. Fujita, Functional molecular flasks: new properties and reactions within discrete, self-assembled hosts, *Angew. Chemie - Int. Ed.*, 2009, **48**, 3418–3438.
3 O. Dumele, N. Trapp and F. Diederich, Halogen Bonding Molecular Capsules, *Angew. Chemie - Int. Ed.*, 2015, **54**, 12339–12344.
4 B. T. Birchall, C. S. Frampton, G. J. Schrobilgen and J. Valsdóttir, b-Hydroquinone Xenon Clathrate, *Acta Cryst.*, 1989, **C45**, 944–946.
5 J. C. a. Boeyens and J. a. Pretorius, X-ray and neutron diffraction studies of the hydroquinone clathrate of hydrogen chloride, *Acta Crystallogr. Sect. B Struct. Crystallogr. Cryst. Chem.*, 1977, **33**, 2120–2124.
6 J.-P. Torré, R. Coupan, M. Chabod, E. Pere, S. Labat, A. Khoukh, R. Brown, J.-M. Sotiropoulos and H. Gornitzka, CO2 – Hydroquinone Clathrate: Synthesis, Purification, Characterization and Crystal Structure, *Cryst. Growth Des.*, 2016, **16**, 5330–5338.
7 E. Eikeland, M. K. Thomsen, J. Overgaard, M. A. Spackman and B. B. Iversen, Intermolecular Interaction Energies in Hydroquinone Clathrates at High Pressure, *Cryst. Growth Des.*, 2017, **17**, 3834–3846.
8 M. Ilczyszyn, M. Selent and M. M. Ilczyszyn, Participation of xenon guest in hydrogen bond network of β-hydroquinone crystal, *J. Phys. Chem. A*, 2012, **116**, 3206–3214.
9 P. Mal, B. Breiner, K. Rissanen and J. R. Nitschke, White phosphorus is air-stable within a self-assembled tetrahedral capsule., *Science*, 2009, **324**, 1697–9.
10 S. H. A. M. Leenders, R. Gramage-Doria, B. de Bruin and J. N. H. Reek, Transition metal catalysis in confined spaces, *Chem. Soc. Rev.*, 2015, **44**, 433–448.
11 N. Ahmad, H. A. Younus, A. H. Chughtai and F. Verpoort, Metal–organic molecular cages: applications of biochemical implications, *Chem. Soc. Rev.*, 2015, **44**, 9–25.
12 R. Wyler, J. de Mendoza and J. Rebek, A Synthetic Cavity Assembles Through Self-Complementary Hydrogen Bonds, *Angew. Chemie Int. Ed. English*, 1993, **32**, 1699–1701.
13 T. Szabo, G. Hilmersson and J. J. Rebek, Dynamics of Assembly and Guest Exchange in the Tennis Ball, *J. Am. Chem. Soc.*, 1998, **120**, 6193–6194.
14 F. Hof, L. C. Palmer and J. J. Rebek, Synthesis and Self-Assembly of the Tennis Ball and Subsequent Encapsulation of Methane, *J. Chem. Ed.*, 2001, **78**, 1519–1521.
15 D. Tzeli, G. Theodorakopoulos, I. D. Petsalakis, D. Ajami and J. Rebek, Theoretical study of hydrogen bonding in homodimers and heterodimers of amide, boronic acid, and carboxylic acid, free and in encapsulation complexes, *J. Am. Chem. Soc.*, 2011, **133**, 16977–16985.
16 D. Tzeli, I. D. Petsalakis, G. Theodorakopoulos, D. Ajami and J. Rebek, Theoretical study of free and encapsulated carboxylic acid and amide dimers, *Int. J. Quantum Chem.*, 2013, **113**, 734–739.
17 L. R. MacGillivray and J. L. Atwood, Achiralsphericalmolecular assemblyheldtogetherby 60 hydrogenbonds, *Nature*, 1997, **389**, 469–472.
18 J. L. Atwood, L. J. Barbour and A. Jerga, Organization of the interior of molecular capsules by hydrogen bonding., *Proc. Natl. Acad. Sci. U. S. A.*, 2002, **99**, 4837–41.
19 G. M. Whitesides, E. E. Simanek, J. P. Mathias, C. T. Seto, D. N. Chin, M. Mammen and D. M. Gordon, Noncovalent synthesis: using physical-organic chemistry to make aggregates, *Acc. Chem. Res.*, 1995, **28**, 37–44.
20 J. M. C. A. Kerckhoffs, M. G. J. Ten Gate, M. A. Mateos-Timoneda, F. W. B. Van Leeuwen, B. Snellink-Ruël, A. L. Spek, H. Kooijman, M. Crego-Calama and D. N. Reinhoudt, Selective self-organization of guest molecules in self-assembled molecular boxes, *J. Am. Chem. Soc.*, 2005, **127**, 12697–12708.
21 S. Kosiorek, B. Rosa, T. Boinski, H. Butkiewicz, M. P. Szymański, O. Danylyuk, A. Szumna and V. Sashuk, Pillar[4]pyridinium: A square-shaped molecular box, *Chem. Commun.*, 2017, **53**, 13320–13323.
22 T. D. Della and C. H. Suresh, Anion Encapsulated Fullerenes Behave as Large Anions: A DFT Study, *Phys. Chem. Chem. Phys.*, , DOI:10.1039/C8CP03615B.
23 M. B. Hillyer, H. Gan and B. C. Gibb, Precision Switching in a Discrete Supramolecular Assembly: Alkali Metal Ion-Carboxylate Selectivities and the Cationic Hofmeister Effect, *ChemPhysChem*, 2018, **19**, 2285–2289.
24 M. F. Zalazar, E. N. Paredes, G. D. Romero Ojeda, N. D. Cabral and N. M. Peruchena, Study of Confinement and Catalysis Effects of the Reaction of Methylation of Benzene by Methanol in H-Beta and H-ZSM-5 Zeolites by Topological Analysis of Electron Density, *J. Phys. Chem. C*, 2018, **122**, 3350–3362.
25 O. Shameema, C. N. Ramachandran and N. Sathyamurthy, Blue shift in X-H stretching frequency of molecules due to confinement, *J. Phys. Chem. A*, 2006, **110**, 2–4.
26 R. Musat, J. P. Renault, M. Candelaresi, D. J. Palmer, S. Le Caër, R. Righini and S. Pommeret, Finite size effects on hydrogen bonds in confined water, *Angew. Chemie - Int. Ed.*, 2008, **47**, 8033–8035.
27 M. J. Frisch, G. W. Trucks, H. B. Schlegel, G. E. Scuseria, M. A. Robb, J. R. Cheeseman, J. A. J. Montgomery, T. Vreven, K. N. Kudin, J. C. Burant, J. M. Millam, S. S. Iyengar, J. Tomasi, V. Barone, B. Mennucci, M. Cossi, G. Scalmani and J. A. Reg, 2004.

28 J.-D. Chai and M. Head-Gordon, Long-range corrected hybrid density functionals with damped atom-atom dispersion corrections, *Phys. Chem. Chem. Phys.*, 2008, **10**, 6615–6620.

29 Z. Li, G. Chen, Y. Xu, X. Wang and Z. Wang, Study of the Structural and the Spectral Characteristics of [C3N3(NH2)3]n (n =1-4) Clusters, *J. Phys. Chem. A*, 2013, **117**, 12511–12518.

30 A. N. Petelski, D. J. R. Duarte, S. C. Pamies, N. M. Peruchena and G. L. Sosa, Intermolecular perturbation in the self-assembly of melamine, *Theor. Chem. Acc.*, 2016, **135**, 65.

31 A. N. Petelski, N. M. Peruchena, S. C. Pamies and G. L. Sosa, Insights into the self-assembly steps of cyanuric acid toward rosette motifs: a DFT study, *J. Mol. Model.*, 2017, **23**, 263.

32 C. Fonseca Guerra, H. Zijlstra, G. Paragi and F. M. Bickelhaupt, Telomere Structure and Stability: Covalency in Hydrogen Bonds, Not Resonance Assistance, Causes Cooperativity in Guanine Quartets, *Chem. - A Eur. J.*, 2011, **17**, 12612–12622.

33 S. F. Boys and F. Bernardi, The calculation of small molecular interactions by the differences of separate total energies. Some procedures with reduced errors, *Mol. Phys.*, 1970, **19**, 553–559.

34

35 R. F. W. Bader, M. T. Caroll, J. R. Cheeseman and C. Chang, Properties of atoms in molecules: atomic volumes, *J. Am. Chem. Soc.*, 1987, **109**, 7968–7979.

36 P. Su and H. Li, Energy decomposition analysis of covalent bonds and intermolecular interactions, *J. Chem. Phys.*, 2009, **131**, 014102.

37 M. W. Schmidt, K. K. Baldridge, J. A. Boatz, S. T. Elbert, M. S. Gordon, J. H. Jensen, S. Koseki, N. Matsunaga, K. A. Nguyen, S. Su, T. L. Windus, M. Dupuis and J. A. Montgomery, General Atomic and Molecular Electronic Structure System, *J. Comput. Chem.*, 1993, **14**, 1347–1363.

38 T. Steiner, The Hydrogen Bond in the Solid State, *Angew. Chemie Int. Ed.*, 2002, **41**, 48–76.

39 D. N. Lande and S. P. Gejji, Exploring Chimeric Calix[4]tetrolarene Molecular Scaffolds: Theoretical Investigations, *J. Phys. Chem. A*, 2018, **122**, 4189–4197.

40 P. Murphy, S. J. Dalgarno and M. J. Paterson, Transition Metal Complexes of Calix[4]arene: Theoretical Investigations into Small Guest Binding within the Host Cavity, *J. Phys. Chem. A*, 2016, **120**, 824–839.

41 C. F. Matta, J. Hernández-Trujillo, T. H. Tang and R. F. W. Bader, Hydrogen - Hydrogen bonding: A stabilizing interaction in molecules and crystals, *Chem. - A Eur. J.*, 2003, **9**, 1940–1951.

42 F. H. Allen, C. M. Bird, R. S. Rowland and P. R. Raithby, Resonance-Induced Hydrogen Bonding at Sulfur Aeceptors in R1R2C=S and R1CS2 Systems, *Acta Crystallogr. Sect. B*, 1997, **53**, 680–695.

43 A. Frontera, F. Saczewski, M. Gdaniec, E. Dziemidowicz-Borys, A. Kurland, P. M. Dey??, D. Qui??onero and C. Garau, Anion-?? interactions in cyanuric acids: A combined crystallographic and computational study, *Chem. - A Eur. J.*, 2005, **11**, 6560–6567.

44 A. O. Ortolan, I. Østrøm, G. F. Caramori, R. L. T. Parreira, E. H. Da Silva and F. M. Bickelhaupt, Tuning Heterocalixarenes to Improve Their Anion Recognition: A Computational Approach, *J. Phys. Chem. A*, 2018, **122**, 3328–3336.

45 A. O. Ortolan, G. F. Caramori, F. Matthias Bickelhaupt, R. L. T. Parreira, A. Muñoz-Castro and T. Kar, How the electron-deficient cavity of heterocalixarenes recognizes anions: Insights from computation, *Phys. Chem. Chem. Phys.*, 2017, **19**, 24696–24705.

46 R. F. W. Bader, A Bond Path: A Universal Indicator of Bonded Interactions, *J. Phys. Chem. A*, 1998, **102**, 7314–7323.

47 F. Guo, E. Y. Cheung, K. D. M. Harris and V. R. Pedireddi, Contrasting Solid-State Structures of Trithiocyanuric Acid and Cyanuric Acid, *Cryst. Growth Des.*, 2006, **6**, 846–848.

48 E. L. Angelina, D. J. R. Duarte and N. M. Peruchena, Is the decrease of the total electron energy density a covalence indicator in hydrogen and halogen bonds?, *J. Mol. Model.*, 2013, **19**, 2097–106.

49 D. J. R. Duarte, G. L. Sosa and N. M. Peruchena, Nature of halogen bonding. A study based on the topological analysis of the Laplacian of the electron charge density and an energy decomposition analysis., *J. Mol. Model.*, 2013, **19**, 2035–41.

50 N. J. M. Amezaga, S. C. Pamies, N. M. Peruchena and G. L. Sosa, Halogen bonding: a study based on the electronic charge density., *J. Phys. Chem. A*, 2010, **114**, 552–562.

51 J.-W. Zou, M. Huang, G.-X. Hu and Y.-J. Jiang, Toward a uniform description of hydrogen bonds and halogen bonds: correlations of interaction energies with various geometric, electronic and topological parameters, *RSC Adv.*, , DOI:10.1039/C6RA27590G.

52 C. F. Guerra, J. Handgraaf, E. J. A. N. Baerends, F. M. Bickelhaupt, A. T. Chemie, S. Laboratorium and D. V. Universiteit, Voronoi Deformation Density (VDD) Charges : Assessment of the Mulliken , Bader , Hirshfeld , Weinhold , and VDD, *J. Comput. Chem.*, 2003, **25**, 189–210.

53 F. Cortés-Guzmán and R. F. W. Bader, Complementarity of QTAIM and MO theory in the study of bonding in donor – acceptor complexes, *Coord. Chem. Rev.*, 2005, **249**, 633–662.

